

Mechanical stability of retained austenite during plastic deformation of super high strength carbide free bainitic steels

C. Garcia-Mateo · F. G. Caballero ·
J. Chao · C. Capdevila · C. Garcia de Andres

Received: 2 April 2009 / Accepted: 22 June 2009 / Published online: 16 July 2009
© Springer Science+Business Media, LLC 2009

Abstract New carbide free bainitic microstructures are gaining an increasing interest on behalf the scientific and industrial community. The excellent combination of mechanical properties achieved in those microstructures with no need of complex heat treatments or thermomechanical processes represents their main advantage. The strength is mainly achieved by means of the very fine bainitic ferrite plates, consequence of the transformation mechanism, but the parameters contributing to the ductility of those microstructures are still unclear in this type of microstructures, where a soft phase, retained austenite, is imbedded in a very strong matrix of bainitic ferrite. A priori is reasonable to assume that retained austenite will control the levels of ductility achieved. Further enhancement of ductility can be achieved by the transformation of retained austenite into martensite (strain or stress assisted), thus its mechanical stability plays an important role in the final ductility. In this study, by means of X-ray analysis of interrupted compression tests, it is studied the influence that different microstructural aspects of retained austenite may have on its mechanical stability.

Introduction

Carbide free bainitic microstructures are regarded in this study as a mixture of fine bainitic ferrite plates, retained austenite and some martensite. The aggregates of plates are

called sheaves, whereas the plates within each sheaf are defined as subunits; the subunits within the same sheaf share a common crystallographic orientation. In discussing the morphology of the austenite remaining after transformation to bainite, it is necessary to distinguish between the blocky morphology, bounded by crystallographic variants of bainite sheaves and exhibiting triangular shape in two dimensional sections, and the films of austenite which are retained between the subunits within a given sheaf of bainite. Carbide precipitation is avoided by the judicious use of silicon as an alloying element. This mixed microstructure presents an excellent balance of mechanical properties [1]. Due to the absence of fine carbides, the steels have a high resistance to cleavage fracture and void formation. Then, there is the possibility of improving simultaneously the strength and toughness because of the fine grain size of the bainitic ferrite plates and of further enhancing the ductility by the transformation of the retained austenite into martensite, strain or stress assisted, that increases the strain-hardening rate.

It is believed that ductility in these microstructures is controlled by the amount of retained austenite [2], which is a ductile phase when compared with bainitic ferrite and martensite. As further improvement of ductility can be achieved by transformation to martensite, retained austenite mechanical stability (or its capability to transform to martensite under strain or stress) must be controlled. In this sense, the effect of the chemical composition, morphology and dislocation state on the mechanical stability of this phase is analyzed in this study.

Material and experimental procedure

The chemical composition of the alloy used in this study is listed in Table 1, and it is the result of theoretical design,

C. Garcia-Mateo (✉) · F. G. Caballero · J. Chao ·
C. Capdevila · C. Garcia de Andres
MATERIALIA Research Group, Department of Physical
Metallurgy, Centro Nacional de Investigaciones Metalurgicas
(CENIM-CSIC), Avda. Gregorio del Amo, 8, E 28040 Madrid,
Spain
e-mail: cgm@cenim.csic.es

Table 1 Chemical composition in wt%

C	Si	Mn	Cr	Mo	Co
0.28	1.50	2.04	1.50	0.24	1.48

by means of phase transformation theory alone [3], in order to obtain carbide free bainitic microstructures after hot rolling practice. A 60 kg laboratory heat was elaborated in a pilot plant at ArcelorMittal Research (Maizières les Metz-France) in a vacuum induction furnace under inert atmosphere (Ar, N₂). The generator power was 80 kW. Pure (>99.9%) electrolytic iron and addition of the alloying elements one after each other were used. Carbon deoxidation was performed and an analysis of C, S, N, O was made on line during elaboration for the final adjustment of composition. During elaboration, the temperature was controlled by a thermocouple. Hot rolling simulations were also performed in the above mentioned facilities, where lumps of the ingot were submitted to the route presented in Fig. 1. After hot rolling an accelerated cooling is applied in order to avoid the formation of proeutectoid ferrite, then the desired bainitic microstructure was obtained by performing from ~500 °C to room temperature air cooling (JT3) or coiling (JT4), the final dimensions of the slabs were 180 × 80 × 12 mm³. Further details on the metallurgical design and industrial processing can be found in Ref. [4, 5].

Sample extraction was always transverse to the hot rolling direction, and standard metallographic techniques were used. A 2% Nital etching solution was used to reveal bainitic microstructure by optical and scanning electron microscopy. Scanning electron microscopy observation was carried out on a Jeol JSM-6500F field emission gun scanning electron microscope operating at 7 kV. Quantitative X-ray diffraction analysis was used to determine the fraction of retained austenite (V_γ) and its carbon content. For this purpose, samples were machined, grinded and finally

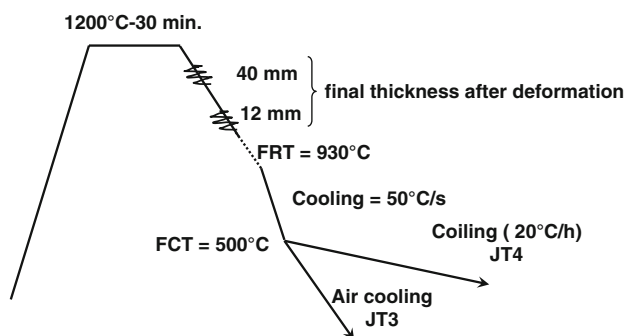


Fig. 1 Route of the performed hot rolling simulation, where *FRT* stands for the finish rolling temperature, and *FCT* for the finishing cooling temperature

polished using 1 μm diamond paste, samples were lightly etched to obtain an undeformed surface. They were then step-scanned in a SIEMENS D 5000 X-ray diffractometer using unfiltered CoK_α radiation. The scanning speed (2θ) was less than 0.3°/min. The machine was operated at 40 kV and 30 mA. The volume fraction of retained austenite was calculated from the integrated intensities of (200), (220) and (311) austenite peaks, and those of (002), (112) and (022) planes of ferrite. Then the amount of martensite/austenite constituent (V_{MA}) was determined by point counting on scanning electron micrographs, being the fraction of martensite $V_\alpha' = V_{MA} - V_\gamma$ and that of bainitic ferrite $V_{zb} = (1 - V_\gamma - V_\alpha')$.

Moreover, retained austenite composition was calculated making use of the relationship between lattice parameter and chemical composition as reported in Ref. [6, 7], this relationship has been selected for being the most complete in terms of the influence of different elements in the austenite lattice parameter. Thus, making use of the austenite lattice parameter obtained by X-ray it is possible to work out the C concentration just by considering that for bainite transformation, nucleation takes place under para-equilibrium conditions (only C diffuses) and its growth is diffusionless [8]. In other words, the concentration ratios of all elements except C should be equal in the bulk material as in the retained austenite (γ) i.e. $(x_{Fe}/x_j)_{bulk} = (x_{Fe}/x_j)_\gamma$, where j denotes any substitutional element in the alloy, and x_{Fe} and x_j are the concentrations of Fe and of the substitutional elements, respectively.

For the tensile test, specimens had a section of 3 mm diameter and a gauge length of 19 mm, while for compression tests the specimens had 4 mm diameter and 6 mm length. Tensile tests were performed according to the UNE EN 10.002_1 standard and assisted by an extensometer. All experiments, compression and tensile, were conducted at room temperature using a Microtest EM2/100/FR testing machine fitted with a 100 kN load cell. A deformation rate of $6 \times 10^{-4} \text{ s}^{-1}$ was used in all the experiments. From the engineering stress–strain curves, offset yield strength ($YS_{0.2}$) and ultimate tensile strength (UTS) were obtained. The uniform (ϵ_u) deformation was obtained from the true stress–strain curves. Strain hardening was characterized by the incremental strain-hardening exponent $n_i = d(\ln\sigma)/d(\ln\epsilon_p)$ obtained from the true stress–true plastic strain curve. The calculation of the factor n_i is extremely sensitive, and in high strength materials the use of an extensometer during testing is compulsory in order to report an accurate value. As for compression tests, extensometer was not available, therefore the use of tensile tests is justified in this work.

The necessary thermodynamic calculations were performed by means of MTDATA with the NPL-plus data base for steels [9].

Results and discussion

Experimental quantitative data presented in Table 2 shows that regardless of the applied cooling path the microstructure is mainly bainitic, with bainitic ferrite volume fractions as high as 85%, the remaining being austenite and martensite in different quantities. SEM micrographs in Fig. 2 illustrate that bainite sheaves are formed by very thin and long parallel bainitic ferrite plates and martensite/austenite (MA) constituent, where the extraordinary small size of the MA grains inside bainite sheaves is also evident.

Film and blocky austenite fractions can be deduced from the total fraction of retained austenite determined by X-ray

Table 2 Quantitative data on microstructure at room temperature after air cooling (JT3) and coiling (JT4)

	V_{zb}	$V_{\alpha'}$	V_{γ} (films)	V_{γ} (blocky)
JT3	85 ± 2	7 ± 4	8 ± 1	–
JT4	77 ± 1	3 ± 2	12 ± 3	8 ± 3

V_{zb} is the volume fraction of bainitic ferrite, $V_{\alpha'}$ is the volume fraction of martensite, V_{γ} is the volume fraction of retained austenite

analysis following Ref. [10], where the authors estimated that about 15% of the volume contained within the boundaries of a bainite sheaf consists of retained austenite films interspersed with bainitic ferrite subunits. Hence, the ratio of the volume fraction of the film type retained austenite V_{γ} (films) to that of the blocky type austenite V_{γ} (blocky) can be deduced from the following expression, V_{γ} (films)/ V_{γ} (blocky) = $(0.15 V_{zb}) / (V_{\gamma} - 0.15 V_{zb})$. In this study, retained austenite in JT3 is only present as thin films between the subunits of bainitic ferrite because of the high volume fraction of bainitic ferrite, while JT4 also exhibits a small fraction of blocky retained austenite, 8%.

Table 3 shows the calculated retained austenite chemical composition following the procedure formerly described. Results thus obtained clearly indicate that the main difference in composition between retained austenite in JT3 and JT4 is the C content. Natural consequence of the diffusionless growth of ferrite is that once it stops growing the excess of C trapped within diffuses to the parent austenite, therefore the higher the fraction of bainitic ferrite is the higher retained austenite C content is. Therefore, austenite C content in JT4 is lower than that measured in JT3.

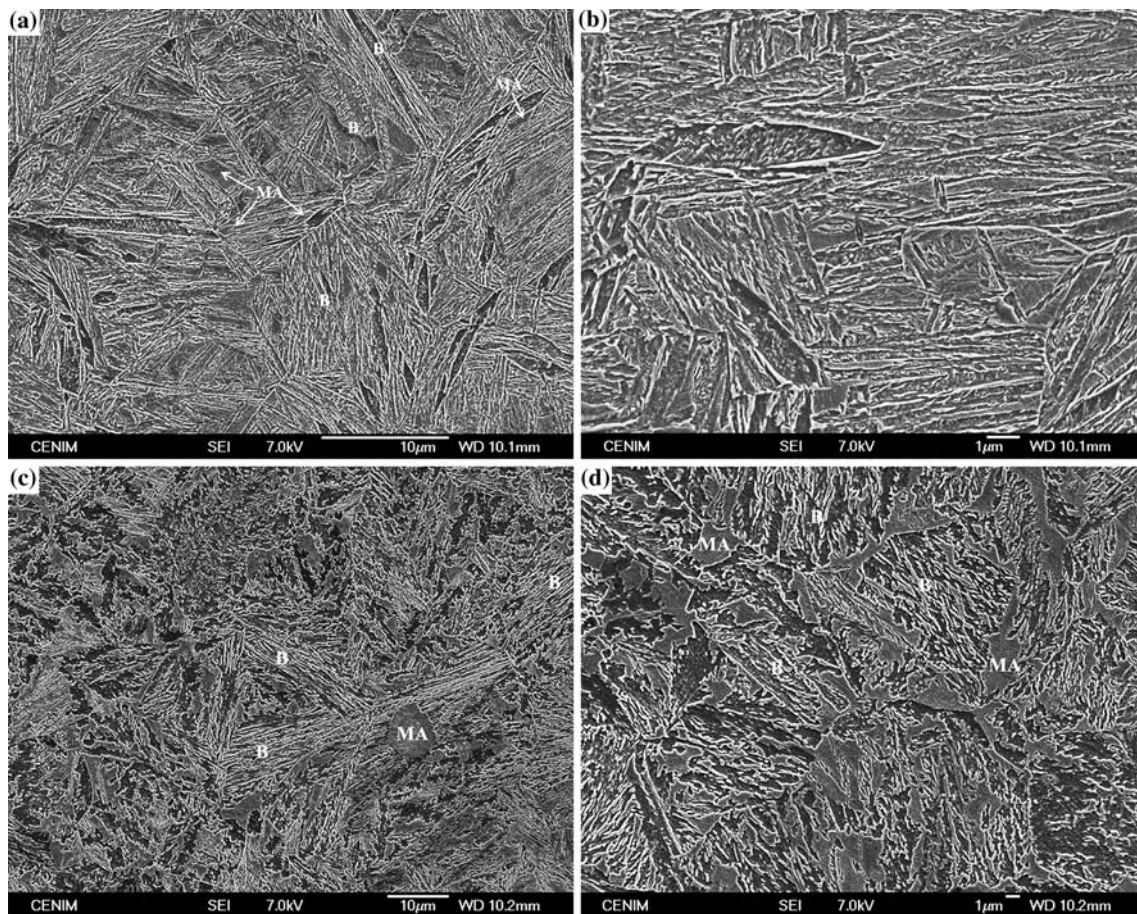


Fig. 2 Scanning electron micrographs of the microstructure revealed a room temperature after: air cooling (JT3) (a) and (b), and coiling (JT4) (c) and (d). B stands for bainite, M for martensite and A for austenite

Table 3 Retained austenite chemical composition in wt%, calculated as described in Ref. [8]

	C	Si	Mn	Cr	Mo	Co	$\Delta G^{\gamma/\alpha}/\text{J mol}^{-1}$
JT3	1.38	1.48	2.02	1.48	0.25	1.46	−1738
JT4	0.81	1.49	2.03	1.49	0.25	1.47	−3039

$\Delta G^{\gamma/\alpha}$ represents the chemical free energy change for transformation of austenite to martensite with no change in chemical composition

But results in Table 2 show that austenite in JT4 seems to have a thermal stability higher than in JT3, smaller fraction of martensite. This is explained by the fact that thin films of retained austenite trapped between bainite plates can host C in higher quantities [11–13]. Moreover, it should be highlighted the fact that X-ray is a ‘bulk’ analysis in the sense that C content estimation by means of this technique is an average of regions of the material that may contain carbon enriched regions such as dislocations and phase interfaces, which are very distinctive features of this type of microstructures [14].

Micrographs in Fig. 2 reveal some other differences between JT3 and JT4 microstructures. JT3 exhibits thin ($\sim 0.3 \mu\text{m}$), long and slender well defined plates, very distinctive of high strength high toughness bainitic steels [15–17] meanwhile the nature of bainite after coiling, JT4, clearly seems to be coarser ($\sim 1.5 \mu\text{m}$). It is well known that by lowering the transformation temperature at which bainite forms an important refinement in the plate thickness of ferritic bainite is achieved [3, 18]. As JT3 was submitted to a much faster cooling rate than JT4, therefore transforming at lower temperatures, so it exhibits a thinner, longer and slender well defined plates when compared with the microstructure obtained after coiling, JT4.

It is also detectable that retained austenite distribution within the bainitic ferrite matrix is different. Usually blocky retained austenite is described as triangular shaped grains bounded by crystallographic variants of bainite sheaves [10], but in JT4 case it is better described as very thick films of austenite between the coarse subunits within a given sheaf of bainite, see Fig. 2d. All those morphological differences can only correspond to differences in the cooling rates applied, and therefore to different transformation temperatures.

It is not strange that such differences between both microstructures, JT3 and JT4, have also lead to different mechanical behaviour and properties. Table 4 gathers the average results obtained from two tensile tests per condition. JT3 shows higher $YS_{0.2}$ and UTS than JT4, and this can be explained if we bear in mind that the main contribution to bainite strength arises from the extremely fine plate thickness of bainitic ferrite [15]. JT3 contains a higher fraction of bainitic ferrite, Table 2, composed of thinner plates than JT4, see Fig. 2.

Table 4 Tensile properties results

	$YS_{0.2}/\text{MPa}$	UTS/MPa	$\epsilon_u/\%$
JT3	1430	1862	3.1
JT4	951	1551	10

However, on the other hand, it is difficult to assess the effect that retained austenite has on strength. Qualitatively, austenite can affect the strength in several ways; residual austenite can transform to martensite during cooling to room temperature, thus increasing the strength. But also, retained austenite interlath films can increase the strength by transforming to martensite during testing, similar to the behaviour of TRIP steels. Tensile strain, a priori is controlled by the volume fraction of retained austenite, which is a ductile phase compared to the bainitic ferrite and it would be expected to enhance ductility as far as the austenite is homogeneously distributed in the microstructure.

Figure 3a, b shows the true strain–stress curves from tensile tests in these microstructures. Where it is possible to appreciate that JT3 has higher strength levels than JT4, but lower ϵ_u . Work hardening behaviour, represented as the incremental work hardening exponent n as a function of true plastic strain has been also represented in Fig. 3c, d. The straight line represents the instability criterion $\epsilon_p = n$. The results reveal very different behaviours when comparing both microstructures. Thus, JT3 shows a very rapid strain hardening increase at early strain stages. However, as true strain increases the strain hardening tends to quickly decrease, while in the case of JT4 after an initial increase of n there is a more gentle decrease up to the fulfilment of the instability criterion. Moreover, the strain hardening capacity near instability of JT4 is higher than that of JT3.

Knowing that there is a correlation between the shape of n curves and the rate at which retained austenite transforms to martensite [8, 19–21], the interpretation of curves in Fig. 3c, d could be as follows: in the case of JT3 there is a rapid transformation of austenite into martensite, at early stages, and it is not possible to get full advantage of the augmentation of ductility consequence of the austenite to martensite transformation, strain or stress assisted. But, in the case of JT4 this same transformation proceeds progressively until the instability criterion is reached and the increment in strain hardening thus obtained enhances ductility.

To prove these asseverations, samples of interrupted compression tests at different plastic strains were analyzed by means of X-ray in order to disclose the evolution of retained austenite fraction. Figure 4a, b shows the complete flow curves of compression tests up to the uniform deformation obtained from tensile tests, Table 4. The shape of the curves is almost identical to those obtained in tensile test,

Fig. 3 Tensile true strain–stress curves of **a** JT3 and **b** JT4, and **c** and **d** the corresponding incremental work hardening exponent, n , as a function of true plastic strain and stress. Straight line represents the instability criterion, i.e. $\epsilon_p = n$

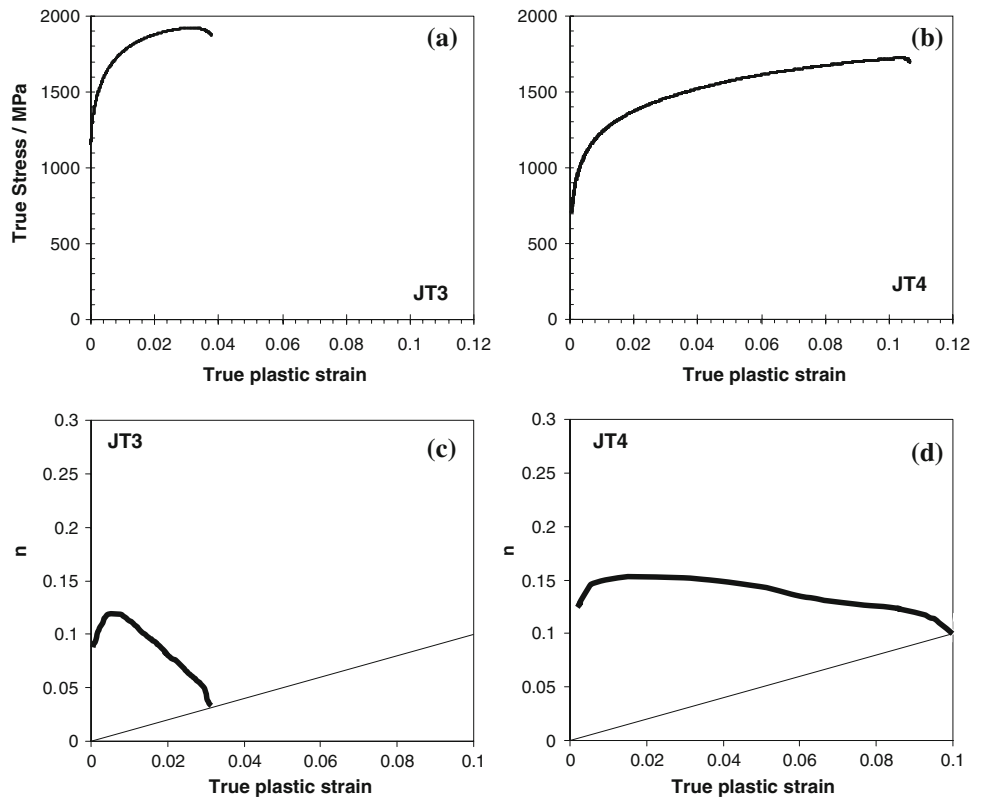


Fig. 4 Compression true strain–stress curves of **a** JT3 and **b** JT4, **c** and **d** fraction of remaining retained austenite after compression tests at different plastic strains. *Open symbols* represent the fraction of retained austenite measured in the uniformly deformed region of the tested tensile specimens. *Dotted line* represents the level of uniform deformation achieved in tensile tests

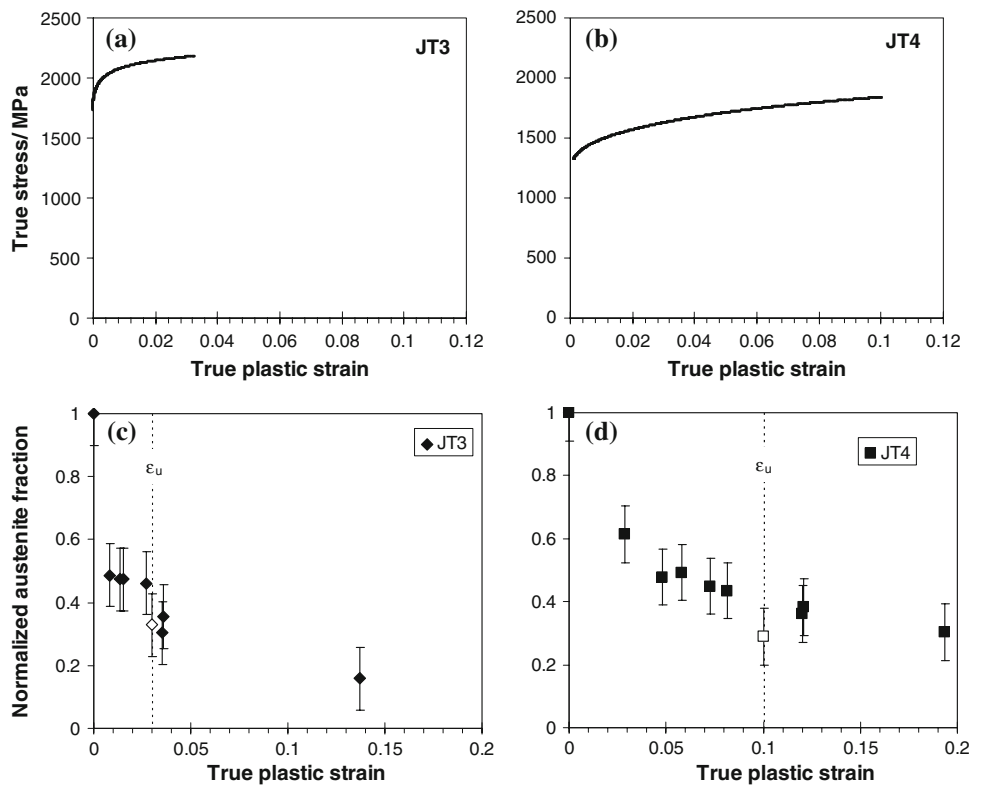


Fig. 3, which allow us to confirm the validity in comparing compression and tension results. For an easier interpretation of the X-ray results on interrupted compression tests,

Fig. 4c, d, results are presented as the normalized austenite fraction versus true plastic strain, therefore taking into account for the different initial volume fractions of

austenite, Table 2. As open symbols it is also represented the normalized fraction of retained austenite measured in the uniformly deformed region of the tested tensile specimens, within the experimental error the reported fractions of austenite in compression and tension are very similar also supporting the validity of the procedure used in this study, despite the fact that previous study reports on the difference in austenite stability under tension and compression have shown differences, although it has to be noted that those studies are for TRIP-aided and austenitic steels [22] and not for bainitic steels. Data shown in Fig. 4c, d suggest that JT4 exhibits a more progressive transformation of austenite than JT3, as possible explanation to the different shape of the n versus true plastic strain plots in Fig. 3c, d.

The differences found in strain-hardening evolution versus retained austenite fraction can be attributed to the difference in which retained austenite transforms to martensite upon deformation, among others, an important factor affecting such behaviour is the austenite mechanical stability, or its ability to transform to martensite under either strain or stress. The experimental results a priori seem to confirm that bainitic microstructure obtained after coiling, JT4, is mechanically more stable than that contained in the microstructure obtained after air cooling, JT3. An attempt to disclose the reasons why is done in the following paragraphs.

One of the most important factors controlling austenite mechanical stability is its chemical composition, thus elements such as C, Mn, Si and Al [23, 24] significantly enhance the mechanical stability of austenite, among them C is the element that exhibit the strongest influence. The calculated chemical driving force at room temperature for the transformation of austenite into martensite $\Delta G^{\gamma/\alpha}$ (i.e. ferrite of the same chemical composition) [9], see Table 3, clearly implies that JT3 is less prone for such transformation than JT4, in other words, and attending exclusively to the chemical composition, retained austenite in JT3 is mechanically more stable than that of JT4. A more intuitive way of presenting such results is by means of Sherif et al. [25] model, based on a quantitative theory for the strain induced transformation of retained austenite in a class of TRIP-assisted steels. The models allow the progress of austenite transformation to be followed as a function of the plastic strain, chemical composition and the temperature at which the deformation is carried out. The effect of the latter two variables is expressed through the chemical driving force for transformation, which has been introduced into a simple equation for strain induced transformation, $\ln V_{\gamma}^0 - \ln V_{\gamma} = k_1 \Delta G^{\gamma/\alpha} \varepsilon$, where V_{γ}^0 and V_{γ} represent the initial austenite fraction and the remaining fraction, after transformation induced plasticity, respectively, k_1 is a constant and ε is the plastic strain. The model can adequately be used for assessing the austenite mechanical stability in a wide

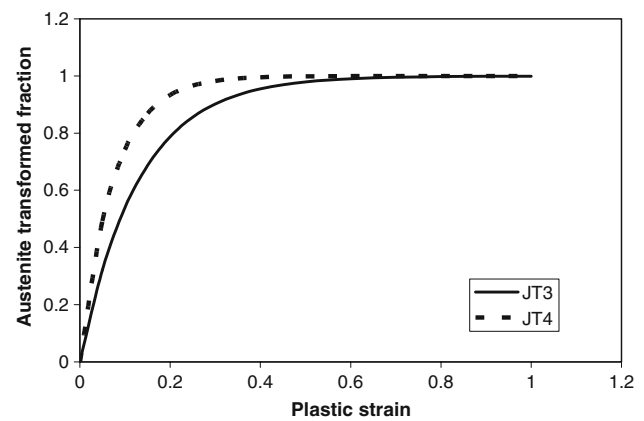


Fig. 5 Theoretical evolution of the transformed fraction of retained austenite as a function of strain [24]

range of TRIP-aided steel and its applicability to bainitic steel has been demonstrated [8, 26]. Results obtained with this model are presented in Fig. 5. It is obvious that the rate of strain assisted transformation from austenite to martensite is much higher in JT4 than in JT3 despite its higher volume fraction of initial retained austenite, and such behaviour can only be attributed to the higher C content in JT3 austenite as compared with that of JT4, see Table 3.

It can be argued that transformation from austenite to martensite is not strain but stress assisted. Figure 6 illustrates ΔG for martensitic transformation in austenites of compositions given in Table 3 for four different stress levels. ΔG takes into account for the chemical ($\Delta G^{\gamma/\alpha}$) and mechanical driving force (ΔG_{MECH}) consequence of applied stress [27]. The effect of stress is to increase the driving force, or to increase the martensite start temperature M_s . Therefore, stress induced martensite may occur when M_s exceeds the temperature at which deformation is carried out, room temperature in our case. Results in Fig. 6 suggest that for the same level of applied stress, in JT4 austenite to martensite stress assisted transformation is more likely than in JT3, with lower ΔG values. If the same levels of plastic strain are considered, e.g. 0 and 0.03 in Fig. 4c, d, the respective stress are 1,700 and 2,100 MPa, respectively, for JT3 and for JT4 1,300 and 1,500 MPa, as it can be seen in Fig. 6 the free energy change in JT4 is at least $1,000 \text{ J mol}^{-1}$, in absolute value, higher than the equivalents in JT3. Again, and according to theory, austenite in JT3 is more stable to martensitic transformation than that of JT4.

Therefore, despite the theoretical results, experiments reveals that retained austenite in JT4 is more stable than in JT3, which rules out that its chemical composition might be controlling its mechanical stability, and for that matter the ductility behaviour.

Beside the chemical composition, morphology of retained austenite is an important factor to be considered on

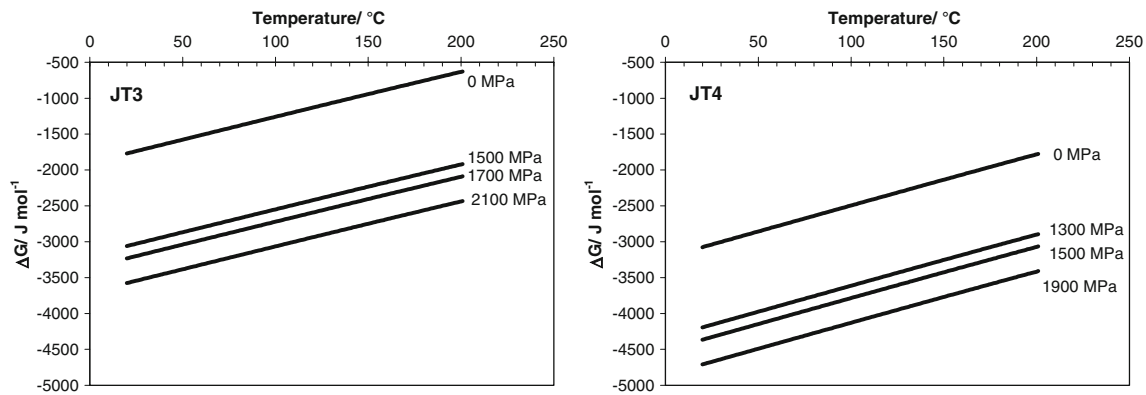


Fig. 6 Total driving force (chemical and mechanical) for austenite to martensite transformation for JT3 and JT4 austenite at different stress levels

its mechanical stability. In terms of its mechanical stability, thin films of retained austenite between bainitic ferrite plates are mechanically more stable, less likely to transform to martensite, in part because of their high carbon concentration [28] and also because of the constraint to transformation exerted by the surrounding plates of ferrite. Thus, comparing the volume fraction of films listed in Table 2, it can be deduced that morphology, in this study, neither is a strong factor for the control of retained austenite mechanical stability. Moreover, and contrary to the traditional belief that isolated pools of austenite (blocky austenite) would influence unfavourably on elongation presumably, because the strain localization in these areas and their lower mechanical stability due to lower C contents, blocky austenite, only present in JT4 microstructure, does not seem to influence unfavourably on its ductility.

Another possibility is that different dislocation densities in JT3 and JT4 are affecting the mechanical stability of retained austenite. As austenite to martensite transformation involves the coordinated movement of atoms, the motion of glissile interfaces becomes impossible when the defect density is high enough, meaning that dislocations present in the microstructure may mechanically stabilize austenite retarding or even impeding martensitic transformation. Two sources of defects are found in our case, first from the thermal transformation of austenite into martensite when cooling at room temperature, and second the bainitic transformation itself. It is well established that the shape change accompanying the growth of a bainitic ferrite plate is plastically accommodated in the austenite beside it, which results in the creation of an intense dislocation debris. The dislocation density created increases as the transformation temperature to bainite decreases [3, 13, 15]. As JT3 was subjected to a much faster cooling rate, therefore transforming at lower temperatures than JT4, and it contains a slightly higher fraction of martensite, it is

logical to assume that dislocation density introduced by means of phase transformation in JT3 must be higher than in JT4. Even though, experimental results prove that austenite to martensite during deformation happens at a higher rate in JT3 than in JT4, Fig. 4c, d, showing that there are no signs of mechanical stabilization. To further support this point, retained austenite fraction measurements were performed in compression test where plastic deformation were well over the ϵ_u , i.e. at 13.9% and 19.4% for JT3 and JT4, respectively. The results, also plotted in Fig. 4c, d, show that signs of mechanical stabilization are only evident in JT4 where the fraction of austenite at 19.4% and 10% (ϵ_u) are almost identical, in the case of JT3 transformation to martensite has proceeded as the plastic deformation was increased.

Therefore, all the results presented suggest that there must be other factors affecting retained austenite mechanical stability. There is only one more factor to be evaluated, and this is the ferrite matrix. According to all the results presented, it is evident that bainitic matrix in JT3 is stronger than in JT4, being the main contributions, a higher fraction of bainitic ferrite, plates with smaller size and a higher dislocation density. Therefore, as it has been pointed out, for the same level of deformation the level of stress and work hardening is much higher in JT3 than in JT4, and it can be speculated that this may alter the way and rate in which retained austenite is plastically deformed prior to its transformation to martensite. Bhadeshia's calculations [29] on the contribution that transformation plasticity makes to the total elongation, suggested that the role of retained austenite per se has been overestimated in explaining the good ductility of TRIP assisted steels. It is likely that bainitic ferrite matrix plays an important role on the plastic deformation of austenite. Bainitic microstructures, as those described in this work, would behave as a composite microstructure formed by a hard phase (bainitic ferrite and

some martensite) and a soft phase (austenite) with a complex, interconnected composite deformation behaviour. This topic is the subject of research in progress.

Conclusions

Two carbide free bainitic microstructures have been investigated in terms of the mechanical stability of retained austenite, a phase which is minority and softer if compared with the bainitic ferrite matrix, representing a very different case to the usual TRIP-assisted steels. Retained austenite microstructural parameters, as volume fraction, morphology, chemical composition and dislocation density, have been analyzed trying to elucidate which was the role that they were playing on controlling its mechanical stability. According to theory none of the above mentioned parameters is responsible for the mechanical stability behaviour detected experimentally. In addition to this, an attempt has been made to explain the transformation by means of stress and not strain assisted, and again theory failed to explain the experimental behaviour detected. It is speculated that differences in the bainitic ferrite matrix strength may play an important role in the austenite to martensite transformation.

Acknowledgements The authors gratefully acknowledge the support of Spanish Ministerio de Ciencia y Tecnología Plan Nacional de I_D_I (2004–2007) funding this research under the contract MAT2007–63873. All of us want to thank to T. Iung and S. Allain (ARCELOR RESEARCH) for manufacturing the designed alloys. We are also extremely grateful to M. J. Santofimia for her contribution to the design and development of these alloys and to M. Arias Ruiz de Larramendi for preliminary mechanical tests performed in these alloys.

References

1. Caballero FG, Santofimia MJ, Capdevila C, García-Mateo C, García de Andrés C (2006) *ISIJ Int* 46:1479
2. Sandvik BPI, Nevalainen HP (1981) *Met Technol* 15:213

3. Bhadeshia HKDH (2001) *Bainite in steels*, 2nd edn. Institute Materials, London
4. Caballero FG, García-Mateo C, Chao J, Santofimia MJ, Capdevila C, García de Andrés C (2008) *ISIJ Int* 48:1256
5. Caballero FG, Santofimia MJ, Garcia-Mateo C, Chao J, Garcia de Andres C (2009) *Mater Des* 30:2077
6. Dyson DJ, Holmes B (1970) *J Iron Steel Inst* 208:469
7. Bhadeshia HKDH, Davis SA, Vitek JM, Reed RW (1991) *Mater Sci Technol* 7:686
8. Garcia-Mateo C, Caballero FG (2005) *Mater Trans JIM* 46:1839
9. MTDATA (2004) *Phase Diagram Calculation Software*. National Physical Laboratory, Teddington, UK
10. Bhadeshia HKDH, Edmonds DV (1983) *Metal Sci* 17:411
11. Caballero FG, García-Mateo C, Santofimia MJ, Miller MK, Garcia de Andres C (2009) *Acta Mater* 57:8
12. Bhadeshia HKDH, Waugh AR (1982) *Acta Metall* 30:775
13. Stone HJ, Peet MJ, Bhadeshia HKDH, Withers PJ, Babu SS, Specht ED (2008) *Proc R Soc A* 464:1009
14. Caballero FG, Miller MK, Babu SS, Garcia-Mateo C (2007) *Acta Mater* 55:381
15. Garcia-Mateo C, Caballero FG (2007) *Int J Mater Res* 98:137
16. Garcia-Mateo C, Caballero FG (2005) *ISIJ Int* 45:1736
17. Caballero FG, Bhadeshia HKDH, Mawella KJA, Jones DG, Brown P (2001) *Mater Sci Technol* 17:517
18. Garcia-Mateo C, Caballero FG, Bhadeshia HKDH (2005) *ISIJ Int* 43:1821
19. Jaques PJ, Girault E, Harlet Ph, Delannay F (2001) *ISIJ Int* 41:1061
20. Itami A, Takahashi M, Ushioda K (1995) *ISIJ Int* 35:1121
21. Sugimoto K, Kobayashi M, Hashimoto S (1992) *Metall Trans* 23A:3085
22. Yu HY, Kai GY, De Jian M (2006) *Mater Sci Eng A* 441:331
23. Jaques PJ, Girault E, Mertens A, Verlinden B, Delanny F (2001) *ISIJ Int* 41:1068
24. Nohara K, Ono Y, Ohashi N (1977) *J ISIJ* 63:212
25. Sherif MY, Garcia-Mateo C, Sourmail T, Bhadeshia HKDH (2004) *Mater Sci Technol* 20:319
26. Sherif MY (2006) *Characterisation and development of nano-structured, ultrahigh strength, and ductile bainitic Steels*. PhD Thesis, University of Cambridge. Available online at <http://www.msm.cam.ac.uk/phase-trans/2000/phd.html>
27. Chatterjee S, Bhadeshia HKDH (2007) *Mater Sci Technol* 23:1101
28. Bhadeshia HKDH, Edmonds DV (1979) *Metall Trans A* 10:895
29. Bhadeshia HKDH (2002) *ISIJ Int* 42:1059